On the Ergodic Rate of Uplink Rate-Splitting Multiple Access

Athanasios P. Chrysologou*, Sotiris A. Tegos*, Panagiotis D. Diamantoulakis*, Nestor D. Chatzidiamantis*, Paschalis C. Sofotasios†, and George K. Karagiannidis*‡

*Dept. of Electrical and Computer Engineering, Aristotle University of Thessaloniki, Thessaloniki, Greece
e-mails: {chrysolog, tegosoti, padiaman, nestoras, geokarag}@auth.gr
†C2PS and 6G Center, Department of Computer and Communication Engineering, Khalifa University, 127 788, Abu Dhabi, UAE
e-mail: paschalis.sofotasios@ku.ac.ae
‡Cyber Security Systems and Applied AI Research Center, Lebanese American University (LAU), Lebanon

2024 IEEE Wireless Communications and Networking Conference (WCNC) | 979-8-3503-0358-2/24/$31.00 ©2024 IEEE | DOI: 10.1109/WCNC57260.2024.10571117

***Abstract*—One of the principal challenges anticipated for the forthcoming sixth-generation (6G) wireless networks is the imperative need to design advanced multiple access techniques capable of enabling massive connectivity. In this direction, rate splitting multiple access (RSMA) has been reported as a promising approach. In this work, we investigate the ergodic rate (ER) performance of an uplink RSMA network which consists of two sources. Specifically, analytical closed-form expressions for the sources' ERs and the system ergodic sum rate (ESR) are derived under the case of perfect successive interference cancellation (pSIC) and perfect channel state information (pCSI) as well as under the more realistic scenario of imperfect SIC (ipSIC) and imperfect CSI (ipCSI). Furthermore, an asymptotic analysis for the high signal-to-noise ratio regime is presented, which provides useful insights into the sources' behavior in all considered cases. The accuracy of the provided analytical expressions is validated by simulation results, which not only explore how different system parameters affect the extracted expressions, but also reveal the detrimental impact of ipSIC and ipCSI on system performance.**

***Index Terms*—Rate splitting multiple access (RSMA), ergodic rate, imperfect successive interference cancellation (SIC), imperfect channel state information (CSI).**

I. Introduction

The upcoming sixth-generation (6G) wireless networks are expected to confront the imperative task of efficiently serving a multitude of devices, sensors, and services, each with diverse and heterogeneous requirements [1]. To ensure such seamless massive access and deliver a superior quality of experience (QoE), it becomes essential to depart from conventional multiple access (MA) schemes and design innovative next generation MA (NGMA) strategies that are capable of addressing the unique challenges of 6G. Recently, rate-splitting multiple access (RSMA) has attracted much attention as a massive access 6G technology, primarily due to its ability to provide a more comprehensive and robust transmission approach compared to non-orthogonal multiple access (NOMA) [2].

A thorough examination of the open literature reveals that the predominant body of research on RSMA mainly concentrates on the downlink. However, as demonstrated in previous works [3], it is noteworthy that the utilization of uplink RSMA allows the attainment of the capacity region of the multiple access channel, thus making the study of uplink RSMA imperative. In this context, the authors of [4] studied the achievable sum rate as well as the outage performance of an uplink two-user RSMA network. For the same system model, [5] proved that the rate-splitting technique is able to improve both fairness and outage performance. Compared to the previous works, which only considered one of many possible message decoding orders, in [6], the outage throughput of uplink RSMA under arbitrary decoding order was investigated. In [7], Lu et al. explored the outage performance of uplink RSMA transmissions in scenarios where users are randomly deployed in the network. Their analysis took into account user scheduling schemes and power allocation strategies. Moreover, the authors of [8] introduced a cooperative RSMA scheme aimed at harnessing the transmit diversity achieved through cooperative transmissions and proved that cooperative RSMA outperforms cooperative NOMA. Furthermore, [9] proposed a cognitive radio (CR)-inspired uplink rate splitting strategy which was proven to maximize the achievable rate of secondary users without adversely affecting the outage performance of primary users. In contrast to the aforementioned works that operated under the assumption of infinite blocklength, [10] assessed the performance boundaries of a two-user single-input single-output system under the assumption of a finite blocklength framework. Finally, in [11], two CR-inspired protocols based on RSMA and NOMA were presented and studied in terms of secondary user's ergodic rate (ER).

Based on the aforementioned technical literature review and to the best of the authors' knowledge, it is observed that the great majority of existing uplink RSMA-oriented works focus on the outage performance investigation or OP minimization, thus leaving the study of users' ER in uplink RSMA networks unexplored. In the meantime, it is noteworthy that all contributions that studied the performance of uplink RSMA have assumed perfect knowledge of channel state information (CSI) as well as perfect successive interference cancellation (pSIC). However, these assumptions are far from real-world scenarios where practical challenges abound and make practical applications suffer from the dual challenges of

imperfect CSI (ipCSI) and imperfect SIC (ipSIC), thus, leading to notable performance degradation [12], [13].

In light of these observations, this work considers an uplink RSMA network and examines its ER performance within the context of practical imperfections. Specifically, the contributions of our work can be summarized as follows:

- We consider an uplink network consisting of a base station (BS) and two wireless sources. Analytical closed-form ER expressions are derived for both sources under the ideal assumption of perfect CSI (pCSI) and pSIC as well as under the more realistic scenario of ipCSI and ipSIC. Additionally, the aforementioned expressions are utilized to extract system ergodic sum rate (ESR).
- To gain deeper insights, a high signal-to-noise ratio (SNR) analysis is conducted. It is revealed that ER floors tend to emerge at high SNRs in most of the cases.
- The accuracy of the extracted expressions is validated via simulations which also reveal the impact of different system parameters on sources' ERs and system ESR under all pCSI, pSIC, ipCSI, ipSIC cases. Furthermore, the detrimental effect of ipCSI and ipSIC on sources' ERs as well as on the system ESR is illustrated, thus underscoring the necessity of considering these practical constraints when examining RSMA-based systems.

II. System Model

We consider an uplink RSMA network consisting of a BS and two wireless sources, denoted as S_1 and S_2, respectively. We assume that all nodes are equipped with a single antenna and we further denote as h_1 and h_2 the channel coefficients between S_1 and the BS, and S_2 and the BS, respectively. Both channel coefficients are assumed to undergo Rayleigh fading, i.e., $h_i \sim \mathcal{CN}(0, \lambda_i)$ with $i \in \{1, 2\}$. In the presence of ipCSI, according to minimum mean squared error (MMSE) estimation [12], it stands

$$h_i = \hat{h}_i + \epsilon_i, \tag{1}$$

where h_i is the actual channel, $\hat{h}_i$ is the estimate of h_i, and ϵ_i is the CEE, which is assumed to be complex normal random variable with zero mean and variance $\sigma^2_{\epsilon_i}$, i.e., $\epsilon_i \sim \mathcal{CN}(0, \sigma^2_{\epsilon_i})$. It is mentioned that the parameter $\sigma^2_{\epsilon_i}$ can be seen as indicator of the channel estimation accuracy. By further assuming that $\hat{h}_i$ and ϵ_i are uncorrelated [14], the estimated channel variance can be given as $\hat{\lambda}_i = \lambda_i - \sigma^2_{\epsilon_i}$.

It has been proven that in order to reach the capacity region of the multiple access channel, splitting the message of only one source is sufficient [4]. Hence, without loss of generality, we assume that only the message of S_1 is split and thus, the message received at the BS can be given as

$$y_B = \sqrt{a_1 P} h_1 x_{11} + \sqrt{a_2 P} h_1 x_{12} + \sqrt{P} h_2 x_2 + n_b, \tag{2}$$

where n_b denotes the additive white Gaussian noise (AWGN) with zero mean and variance N_0 at the BS, P is sources' transmit power, x_{11}, x_{12} are the two parts of S_1's message and a_1, a_2 are the power allocation coefficients for x_{11}, x_{12}, respectively, with $a_1 + a_2 = 1$.

The decoding order that is reported to allow uplink RSMA to reach the capacity region is (x_{11}, x_2, x_{12}) [4], [5]. Hence, invoking (1) in (2), the received signal-to-interference-plus-noise ratio (SINR) at the BS for the detection of message x_{11}, can be modeled as

$$\gamma_{x_{11}} = \frac{a_1 \rho |\hat{h}_1|^2}{\rho \sigma^2_{\epsilon_1} + \rho |\hat{h}_2|^2 + \rho \sigma^2_{\epsilon_2} + a_2 \rho |\hat{h}_1|^2 + 1}, \tag{3}$$

where $\rho = \frac{P}{N_0}$ is sources' transmit SNR. Regarding pSIC, once the BS has successfully decoded x_{11} and by utilizing the channel estimation $\hat{h}_1$, it becomes capable of generating the term $\sqrt{a_1 P}\hat{h}_1 x_{11}$ and completely eliminating it from the received signal y_B given by (2). On the contrary, when ipSIC is applied, the aforementioned term cannot be entirely eliminated from equation (2). Consequently, when attempting to decode x_2, there remains some residual interference due to ipSIC. Similarly, when attempting to decode x_{12} in the presence of ipSIC, there is residual interference caused by the incomplete elimination of both $\sqrt{a_1 P}\hat{h}_1 x_{11}$ and $\sqrt{P}\hat{h}_2 x_2$ from equation (2). As a result, the SINRs at the BS for the decoding of messages x_2 and x_{12} can be respectively expressed as follows:

$$\gamma_{x_2} = \frac{\rho |\hat{h}_2|^2}{\rho \sigma^2_{\epsilon_2} + \rho \sigma^2_{\epsilon_1} + a_2 \rho |\hat{h}_1|^2 + \tilde{k}_1 a_1 \rho |\hat{h}_1|^2 + 1}, \tag{4}$$

$$\gamma_{x_{12}} = \frac{a_2 \rho |\hat{h}_1|^2}{\rho \sigma^2_{\epsilon_1} + \tilde{k}_1 a_1 \rho |\hat{h}_1|^2 + \tilde{k}_2 \rho |\hat{h}_2|^2 + \rho \sigma^2_{\epsilon_2} + 1}, \tag{5}$$

where $\tilde{k}_1$, $\tilde{k}_2$ denote the impact of ipSIC. It is mentioned that $\tilde{k}_i \in [0, 1]$ with $\tilde{k}_i = 0$ denoting pSIC and $\tilde{k}_i = 1$ denoting the no SIC case.

III. Ergodic Rate Analysis

In applications where users' desired data rates adjust dynamically based on their channel conditions, ER emerges as a suitable performance measure. Consequently, in what follows we calculate the ER of both S_1 and S_2.

A. ER of S_1

Source's S_1 ER can be expressed as [11]

$$\begin{aligned} \bar{C}_1 &= \mathbb{E}\{\log_2(1 + \gamma_{x_{11}})\} + \mathbb{E}\{\log_2(1 + \gamma_{x_{12}})\} \\ &\triangleq \bar{C}_{x_{11}} + \bar{C}_{x_{12}}, \end{aligned} \tag{6}$$

where $\mathbb{E}\{\cdot\}$ denotes statistical expectation.

The following theorem returns the ER of source S_1.

Theorem 1. *The ER of S_1 under ipCSI can be given as*

$$\bar{C}_1 = \bar{C}_{x_{11}} + \bar{C}_{x_{12}}, \tag{7}$$

where $\bar{C}_{x_{11}}$, $\bar{C}_{x_{12}}$ are given by (8), (9), respectively, presented at the top of the next page, where $c = \frac{\hat{\lambda}_2 \tilde{k}_2}{\hat{\lambda}_1}$ and $\mathrm{Ei}(\cdot)$ denotes the exponential integral function [15, Eq. (8.211.1)].

Proof: The proof is provided in Appendix A. ∎

Remark 1. *The ER of S_1 under pCSI can be calculated via (7) as soon as $\sigma^2_{\epsilon_1}$, $\sigma^2_{\epsilon_2}$ are set to zero. On the other hand, $\bar{C}_1$ under pSIC cannot be given by just setting $\tilde{k}_1 = \tilde{k}_2 = 0$ in (7).*

$$\bar{C}_{x_{11}} = \begin{cases} -\frac{a_2}{a_1 \ln 2} e^{\frac{D_1}{a_2 \hat{\lambda}_1 \rho}} \mathrm{Ei}\left(-\frac{D_1}{a_2 \hat{\lambda}_1 \rho}\right) + \frac{a_2}{a_1 \ln 2} e^{\frac{D_1}{\hat{\lambda}_1 \rho}} \mathrm{Ei}\left(-\frac{D_1}{\hat{\lambda}_1 \rho}\right) + \frac{a_1}{(1-a_2)\ln 2}\left(\frac{D_1}{\hat{\lambda}_1 \rho} e^{\frac{D_1}{\hat{\lambda}_1 \rho}} \mathrm{Ei}\left(-\frac{D_1}{\hat{\lambda}_1 \rho}\right) + 1\right), & \hat{\lambda}_2 = \hat{\lambda}_1 \\ \frac{1}{a_1 \ln 2} e^{\frac{D_1}{a_2 \hat{\lambda}_1 \rho}} \mathrm{Ei}\left(-\frac{D_1}{a_2 \hat{\lambda}_1 \rho}\right) - \frac{1}{a_1 \ln 2} e^{\frac{D_1}{\hat{\lambda}_1 \rho}} \mathrm{Ei}\left(-\frac{D_1}{\hat{\lambda}_1 \rho}\right) + \frac{a_1}{a_2(a_2-1)\ln 2}\left(\frac{D_1}{\hat{\lambda}_1 \rho} e^{\frac{D_1}{a_2 \hat{\lambda}_1 \rho}} \mathrm{Ei}\left(-\frac{D_1}{a_2 \hat{\lambda}_1 \rho}\right) + a_2\right), & \hat{\lambda}_2 = a_2 \hat{\lambda}_1 \\ -\frac{a_1 \hat{\lambda}_1}{\ln 2}\left(\frac{1}{\hat{\lambda}_2\left(1-\frac{a_2\hat{\lambda}_1}{\hat{\lambda}_2}\right)\left(1-\frac{\hat{\lambda}_1}{\hat{\lambda}_2}\right)} e^{\frac{D_1}{\hat{\lambda}_2 \rho}} \mathrm{Ei}\left(-\frac{D_1}{\hat{\lambda}_2 \rho}\right) + \frac{1}{a_2\left(\hat{\lambda}_1 - \frac{\hat{\lambda}_2}{a_2}\right)\left(1-\frac{1}{a_2}\right)} e^{\frac{D_1}{a_2 \hat{\lambda}_1 \rho}} \mathrm{Ei}\left(-\frac{D_1}{a_2 \hat{\lambda}_1 \rho}\right) \right. \\ \left. \quad + \frac{1}{a_1(\hat{\lambda}_1 - \hat{\lambda}_2)} e^{\frac{D_1}{\hat{\lambda}_1 \rho}} \mathrm{Ei}\left(-\frac{D_1}{\hat{\lambda}_1 \rho}\right)\right), & \text{otherwise} \end{cases} \tag{8}$$

$$\bar{C}_{x_{12}} = \begin{cases} \frac{a_2}{\ln 2(\tilde{k}_1 a_1 - c)}\left(\frac{a_1 \tilde{k}_1}{(\tilde{k}_1 a_1 - c)}\left(e^{\frac{D_1}{c\hat{\lambda}_1 \rho}} \mathrm{Ei}\left(-\frac{D_1}{c\hat{\lambda}_1 \rho}\right) - e^{\frac{D_1}{\tilde{k}_1 a_1 \hat{\lambda}_1 \rho}} \mathrm{Ei}\left(-\frac{D_1}{\tilde{k}_1 a_1 \hat{\lambda}_1 \rho}\right)\right) - \frac{D_1}{c\hat{\lambda}_1 \rho} e^{\frac{D_1}{c\hat{\lambda}_1 \rho}} \mathrm{Ei}\left(-\frac{D_1}{c\hat{\lambda}_1 \rho}\right) - 1\right), & \frac{\hat{\lambda}_2}{\hat{\lambda}_1} = \frac{\tilde{k}_1 a_1 + a_2}{\tilde{k}_2} \\ \frac{\tilde{k}_1 a_1 + a_2}{a_2 \ln 2}\left(e^{\frac{D_1}{\tilde{k}_1 a_1 \hat{\lambda}_1 \rho}} \mathrm{Ei}\left(-\frac{D_1}{\tilde{k}_1 a_1 \hat{\lambda}_1 \rho}\right) - e^{\frac{D_1}{a\hat{\lambda}_1 \rho}} \mathrm{Ei}\left(-\frac{D_1}{a\hat{\lambda}_1 \rho}\right)\right) - \frac{1}{\ln 2}\left(\frac{D_1}{\tilde{k}_1 a_1 \hat{\lambda}_1 \rho} e^{\frac{D_1}{\tilde{k}_1 a_1 \hat{\lambda}_1 \rho}} \mathrm{Ei}\left(-\frac{D_1}{\tilde{k}_1 a_1 \hat{\lambda}_1 \rho}\right) + 1\right), & \frac{\hat{\lambda}_2}{\hat{\lambda}_1} = \frac{\tilde{k}_1 a_1}{\tilde{k}_2} \\ -\frac{a_2 \hat{\lambda}_1}{\ln 2}\left(\frac{1}{\hat{\lambda}_2 \tilde{k}_2\left(1-\frac{\tilde{k}_1 a_1}{c}\right)\left(1-\frac{\tilde{k}_1 a_1 + a_2}{c}\right)} e^{\frac{D_1}{\hat{\lambda}_2 \tilde{k}_2 \rho}} \mathrm{Ei}\left(-\frac{D_1}{\hat{\lambda}_2 \tilde{k}_2 \rho}\right) + \frac{1}{\tilde{k}_1 a_1\left(\hat{\lambda}_1 - \frac{\hat{\lambda}_2 \tilde{k}_2}{\tilde{k}_1 a_1}\right)\left(1-\frac{\tilde{k}_1 a_1 + a_2}{\tilde{k}_1 a_1}\right)} e^{\frac{D_1}{\hat{\lambda}_1 \tilde{k}_1 a_1 \rho}} \right. \\ \left. \quad \times \mathrm{Ei}\left(-\frac{D_1}{\hat{\lambda}_1 \tilde{k}_1 a_1 \rho}\right) + \frac{1}{(\tilde{k}_1 a_1 + a_2)\left(\hat{\lambda}_1 - \frac{\hat{\lambda}_2 \tilde{k}_2}{\tilde{k}_1 a_1} a_2\right)\left(1-\frac{\tilde{k}_1 a_1}{\tilde{k}_1 a_1 + a_2}\right)} e^{\frac{D_1}{\hat{\lambda}_1 \rho(\tilde{k}_1 a_1 + a_2)}} \mathrm{Ei}\left(-\frac{D_1}{\hat{\lambda}_1 \rho(\tilde{k}_1 a_1 + a_2)}\right)\right), & \text{otherwise} \end{cases} \tag{9}$$

In the following lemma, S_1's ER under pSIC is calculated.

Lemma 1. *The ER of S_1 under pSIC can be evaluated as*

$$\bar{C}_1^p = \bar{C}_{x_{11}} - e^{\frac{D_1}{\hat{\lambda}_1 a_2 \rho}} \mathrm{Ei}\left(-\frac{D_1}{\hat{\lambda}_1 a_2 \rho}\right). \tag{10}$$

Proof: The ER of S_1 under pSIC can be evaluated via (7) as soon as $\bar{C}_{x_{12}}$ is properly updated in order to correspond to the pSIC case. Specifically, under pSIC, it holds

$$\bar{C}_{x_{12}}^p = \frac{1}{\ln 2} \int_0^\infty \frac{1 - F_{\gamma_{x_{12}}^p}(x)}{1+x} \mathrm{d}x, \tag{11}$$

where

$$\gamma_{x_{12}}^p = \frac{a_2 \rho |\hat{h}_1|^2}{D_1}. \tag{12}$$

By extracting RV's $\gamma_{x_{12}}^p$ CDF as

$$F_{\gamma_{x_{12}}^p}(x) = F_{|\hat{h}_1|^2}\left(\frac{D_1 x}{a_2 \rho}\right) = 1 - e^{-\frac{D_1 x}{\hat{\lambda}_1 a_2 \rho}}, \tag{13}$$

then invoking (13) in (11) and leveraging [15, Eq. (3.352.4)], (10) occurs. ∎

B. ER of x_2

Regarding S_2, its ER can be given as

$$\bar{C}_2 = \mathbb{E}\{\log_2(1 + \gamma_{x_2})\} \tag{14}$$

The following theorem returns S_2's ER under ipCSI and ipSIC.

Theorem 2. *The ER of S_2 under ipCSI and ipSIC can be calculated as in (15) given at the top of the next page.*

Proof: When it comes to S_2's ER, it holds

$$\bar{C}_2 = \frac{1}{\ln 2} \int_0^\infty \frac{1 - F_{\gamma_{x_2}}(x)}{1+x} \mathrm{d}x. \tag{16}$$

By leveraging (4), we can extract the CDF of RV γ_{x_2} as

$$\begin{aligned} F_{\gamma_{x_2}}(x) &= \Pr\left(\frac{\rho |\hat{h}_2|^2}{a_2 \rho |\hat{h}_1|^2 + \tilde{k}_1 a_1 \rho |\hat{h}_1|^2 + D_1} < x\right) \\ &= \int_0^\infty F_{|\hat{h}_2|^2}\left((a_2 + \tilde{k}_1 a_1)|\hat{h}_1|^2 x + \frac{D_1 x}{\rho}\right) f_{|\hat{h}_1|^2}(y)\, \mathrm{d}y \\ &= 1 - e^{-\frac{D_1 x}{\hat{\lambda}_2 \rho}} \frac{\hat{\lambda}_2}{(a_2 + \tilde{k}_1 a_1)\hat{\lambda}_1 x + \hat{\lambda}_2}. \end{aligned} \tag{17}$$

Applying (17) into (16), yields

$$\bar{C}_2 = \frac{1}{\ln 2} \int_0^\infty \frac{\hat{\lambda}_2}{(1+x)((a_2 + \tilde{k}_1 a_1)\hat{\lambda}_1 x + \hat{\lambda}_2)} e^{-\frac{D_1 x}{\hat{\lambda}_2 \rho}} \mathrm{d}x. \tag{18}$$

If $(a_2 + \tilde{k}_1 a_1)\hat{\lambda}_1 \neq \hat{\lambda}_2$, (18) can be rewritten as

$$\begin{aligned} \bar{C}_2 = \frac{\hat{\lambda}_2}{\ln 2}\Bigg(&\int_0^\infty \frac{e^{-\frac{D_1 x}{\hat{\lambda}_2 \rho}}}{(\hat{\lambda}_2 - (a_2 + \tilde{k}_1 a_1)\hat{\lambda}_1)(1+x)} \mathrm{d}x \\ &+ \int_0^\infty \frac{e^{-\frac{D_1 x}{\hat{\lambda}_2 \rho}}}{\left(1 - \frac{\hat{\lambda}_2}{(a_2 + \tilde{k}_1 a_1)\hat{\lambda}_1}\right)((a_2 + \tilde{k}_1 a_1)\hat{\lambda}_1 x + \hat{\lambda}_2)} \mathrm{d}x\Bigg). \end{aligned} \tag{19}$$

On the contrary, when $(a_2 + \tilde{k}_1 a_1)\hat{\lambda}_1 = \hat{\lambda}_2$, (18) can be transformed into

$$\bar{C}_2 = \frac{1}{\ln 2} \int_0^\infty \frac{1}{(1+x)^2} e^{-\frac{D_1 x}{\hat{\lambda}_2 \rho}} \mathrm{d}x. \tag{20}$$

Applying [15, Eq. (3.352.4)] into (19), [15, Eq. (3.353.3)] in (20) and then combining the resultants (19) and (20), (15) is extracted, and this concludes the proof. ∎

$$\bar{C}_2=\begin{cases}\frac{1}{\ln 2}\left(\frac{D_1}{\hat{\lambda}_2\rho}e^{\frac{D_1}{\hat{\lambda}_2\rho}}\mathrm{Ei}\left(-\frac{D_1}{\hat{\lambda}_2\rho}\right)+1\right), & \hat{\lambda}_2=(a_2+\tilde{k}_1a_1)\hat{\lambda}_1\\ -\frac{1}{\ln 2}\left(\frac{1}{(\hat{\lambda}_2-(a_2+\tilde{k}_1a_1)\hat{\lambda}_1)}e^{\frac{D_1}{\hat{\lambda}_2\rho}}\mathrm{Ei}\left(-\frac{D_1}{\hat{\lambda}_2\rho}\right)+\frac{1}{(a_2+\tilde{k}_1a_1)\hat{\lambda}_1-\hat{\lambda}_2}e^{\frac{D_1}{\hat{\lambda}_1\rho(a_2+\tilde{k}_1a_1)}}\mathrm{Ei}\left(-\frac{D_1}{\hat{\lambda}_1\rho(a_2+\tilde{k}_1a_1)}\right)\right), & \text{otherwise}\end{cases} \tag{15}$$

Remark 2. *The ER of S_2 under pSIC can be evaluated by (15) as soon as $\tilde{k}_1$, $\tilde{k}_2$ are set to zero. Likewise, The ER of S_2 under pCSI can be evaluated via (15) by setting $\sigma^2_{\epsilon_1}$, $\sigma^2_{\epsilon_2}$ equal to zero.*

C. Ergodic Sum Rate

Capitalizing the derived ER expressions of sources S_1 and S_2, system ESR, under ipCSI and ipSIC, can be given as

$$\bar{C}_{\text{sum}}=\bar{C}_1+\bar{C}_2. \tag{21}$$

We note that for the case of pCSI, (21) remains valid as soon as $\sigma^2_{\epsilon_1}$, $\sigma^2_{\epsilon_2}$ are set equal to zero, while for the pSIC scenario, (21) remains valid as soon as $\bar{C}_1$ is replaced with $\bar{C}_1^p$ and $\tilde{k}_1$, $\tilde{k}_2$ are set equal to zero.

D. High SNR regime

In this section, an asymptotic ER analysis for the high SNR regime is conducted.

Lemma 2. *At the high SNR regime, under ipCSI and ipSIC, both S_1 and S_2 show ER floors that can be evaluated via (7), (15), respectively, by replacing D_1 with $\tilde{D}_1=D_1-1$.*

Proof: In (8), (9) and (15), it can be observed that the arguments of both exponential and exponential integral functions have the form: $\frac{GD_1}{B\rho}=\frac{G(D_1-1)+G}{B\rho}$, where G, B are positive constants. It is also noted that (D_1-1) has the form of $(D_1-1)=N\rho$, with N being a positive constant. Hence, at high SNRs, i.e., when $\rho\to\infty$, it holds $\frac{G(D_1-1)+G}{B\rho}\approx\frac{G(D_1-1)}{B\rho}=\frac{GN}{B}$.

It is obvious that the term $\frac{GN}{B}$ is constant and does not depend on ρ, thus, at high SNRs, the ERs of all messages show constant ER floors. This concludes the proof. ∎

Remark 3. *Under ipCSI and pSIC, the ER floor of $\bar{C}_2$ can be given from Lemma 2 as soon as $\tilde{k}_1$, $\tilde{k}_2$ are set to zero. On the other hand, the ER floor of $\bar{C}_1$ can be obtained via (10) as soon as the approximation $\tilde{D}_1=D_1-1$ is used. Conversely, under pCSI and pSIC/ipSIC, the arguments of both exponential and exponential integral functions in (8), (9), (10) and (15) have the form of $\frac{G}{B\rho}$. Hence, applying the approximations $e^{x\to 0}(-x)\approx 1-x$ and $\mathrm{Ei}^{x\to 0}(x)\approx C+\ln(-x)$, where C is the Euler constant, then asymptotic expressions can be obtained.*

IV. Numerical Results and Discussion

In this section, analytical (an.) and simulation (sim.) results are presented to verify the presented analysis as well as to investigate how the different system parameters affect the performance of the presented system model. For the extraction of the following figures, unless otherwise stated, $a_1=0.9$, $\hat{\lambda}_1=2.5$ and $\hat{\lambda}_2=1$ are assumed. Furthermore, for convenience, it is assumed that $\tilde{k}_1=\tilde{k}_2=k$ and $\sigma^2_{\epsilon_1}=\sigma^2_{\epsilon_2}=\sigma^2$.

In Fig. 1, sources' ERs are depicted with respect to the transmit SNR ρ for various σ^2 and k values. First of all, it is obvious that analytical results coincide with the simulation ones, thus, validating the provided analysis. Furthermore, it is illustrated that both sources achieve ER floors at the high SNR regime when ipSIC or ipCSI is applied. More specifically, S_1 achieves an ER floor even if both pSIC and pCSI are assumed, whilst the only case when an ER floor does not appear is the ER of S_1 when pSIC and pCSI are considered. The reason behind those observations are that, as it can be also seen from (3), (4) and (5), the only message that can be decoded under no interference from the other messages or from the SIC, CSI imperfections is x_{12} when pSIC and pCSI are applied. Moreover, despite the fact that under pCSI the decoding of x_{11} is affected by none of the imperfections, the ER of S_1 performance under pCSI, ipSIC appears to be worse compared to the ipCSI, pSIC case. This illustrates the fact that the ipCSI, pSIC conditions are more favorable for x_{12}'s ER than the pCSI, ipSIC conditions. On the other hand, the ER of S_2 under ipCSI and pSIC, i.e., when $k=0.05$, $\sigma^2=0$, appears to obtain higher values compared to the pCSI, ipSIC case, i.e., when $\sigma^2=0.05$, $k=0$.

Fig. 2 depicts the ESR versus transmit SNR ρ for different σ^2 and k values. The high SNR analysis provided in section III-D is further validated as the ER floors and the asymptotic expressions that have been extracted appear to accurately predict the ESR performance at high SNRs. Furthermore, interestingly enough, when comparing the ipCSI, pSIC case with the pCSI, ipSIC one, system ESR shows a similar behavior with S_2's ER, i.e., when $k=0.05$ and $\sigma^2=0$ the ESR achieves higher values than when $\sigma^2=0.05$ and $k=0$.

In Fig. 3, the sources' ERs as well as system ESR with respect to power allocation a_1 can be observed. As expected, as σ^2, k increase, the ER of S_1 and S_2 as well as system ESR decrease. Furthermore, for a fixed set of σ^2, k values, then increased a_1 leads to increased S_2's ER values. This can be explained via (4) which witnesses that a_2 has a stronger effect on γ_{x_2} than a_1 since a_1 is multiplied by k_1. Hence, as a_1 increases, i.e., a_2 decreases, γ_{x_2} increases and that allows the ER of S_2 to achieve higher values. On the other hand, when it comes to S_1, increased a_1 lead to increased γ_{x_1} but decreased $\gamma_{x_{12}}$. Given the fact that, as also from (5) occurs, compared to x_{11}, x_{12} is able to be decoded with less amount of interference form the rest of the messages, then $\gamma_{x_{12}}$ has a stronger impact on S_1's ER than $\gamma_{x_{11}}$. Hence, the ER of S_1 follows $\gamma_{x_{12}}$'s behavior and, thus, is gradually decreased. Finally, when it comes to the pSIC, pCSI case, then the ESR remains constant

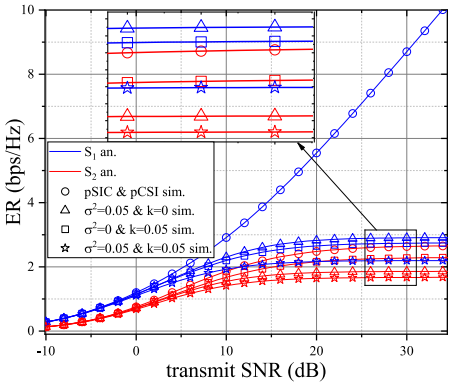

Fig. 1: Sources' ERs vs ρ for different σ^2 and k values.

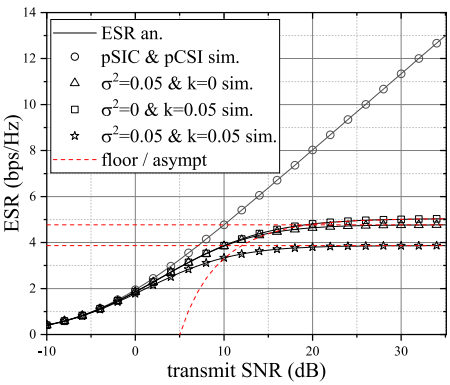

Fig. 2: ESR vs ρ for different σ^2 and k values.

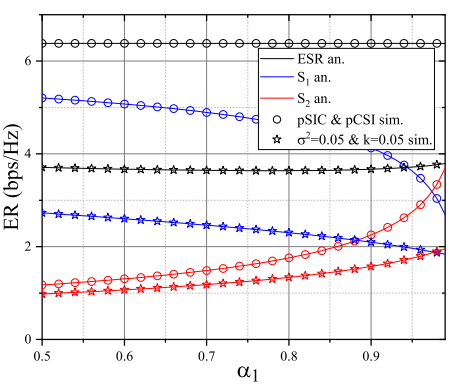

Fig. 3: Sources' ERs and ESR vs a_1 for different σ^2 and k values.

for all a_1 values. This occurs since rate splitting enables the sources to reach the capacity bounds of the multiple access channel. On the contrary, for the ipSIC, ipCSI case, it occurs that the ESR values present a small fluctuation.

V. Conclusion

In this work, we considered a wireless network consisting of a BS and two sources which intent to transmit their messages to the BS exploiting RSMA. For such a setup, we investigated sources' ER performance by deriving closed-form expressions under the ideal case of pSIC, pCSI and the more realistic case of ipCSI, ipSIC. Additionally, an asymptotic ER analysis was conducted, which provided further insights into sources' and system performance at high SNRs. Simulations validated the provided expressions and illustrated the detrimental impact of CSI and SIC imperfections, thus revealing the necessity to include such imperfections in the future studies.

Appendix A
Proof of Theorem 1

In terms of $\bar{C}_{x_{11}}$, it holds

$$\begin{aligned}\bar{C}_{x_{11}} &= \int_0^\infty \log_2(1+\gamma) f_{\gamma_{x_{11}}}(\gamma)\mathrm{d}\gamma \\ &\overset{(\alpha)}{=} \frac{1}{\ln 2}\int_0^\infty \frac{1-F_{\gamma_{x_{11}}}(x)}{1+x}\mathrm{d}x,\end{aligned} \tag{22}$$

where step (α) occurs by leveraging [16, Eq. (28)] and $F_Z(\cdot)$, $f_Z(\cdot)$ denote the the cumulative distribution function (CDF) and probability density function (PDF), respectively, of a random variable (RV) Z.

It becomes evident that in order to further proceed into the calculation of S_1's ER, the CDF of $\gamma_{x_{11}}$ must be extracted. In this direction, considering the definition of CDF, it holds

$$\begin{aligned}F_{\gamma_{x_{11}}}(x) &= \Pr\left(\gamma_{x_{11}} < x\right) \\ &\overset{(\beta)}{=} \Pr\left(\frac{a_1\rho|\hat{h}_1|^2}{\rho|\hat{h}_2|^2 + a_2\rho|\hat{h}_1|^2 + D_1} < x\right) \\ &= \begin{cases}\Pr\left(|\hat{h}_1|^2 < \frac{\rho|\hat{h}_2|^2 x + D_1 x}{a_1\rho - a_2\rho x}\right), & x < \frac{a_1}{a_2} \\ 1, & \text{otherwise,}\end{cases}\end{aligned} \tag{23}$$

where step (β) occurs by invoking (3) and $D_1 = a_1\rho\sigma^2_{\epsilon_1} + \rho\sigma^2_{\epsilon_2} + a_2\rho\sigma^2_{\epsilon_1} + 1$. Focusing on the case when $x < \frac{a_1}{a_2}$, then

$$\begin{aligned}F_{\gamma_{x_{11}}}(x) &= \int_0^\infty F_{|\hat{h}_1|^2}\left(\frac{\rho x y + D_1 x}{a_1\rho - a_2\rho x}\right) f_{|\hat{h}_2|^2}(y)\,\mathrm{d}y \\ &= 1 - \frac{1}{\hat{\lambda}_2} e^{-\frac{D_1 x}{\hat{\lambda}_1\rho(a_1 - a_2 x)}} \int_0^\infty e^{-y\left(\frac{1}{\hat{\lambda}_2} + \frac{x}{\hat{\lambda}_1(a_1 - a_2 x)}\right)}.\end{aligned} \tag{24}$$

By performing the exponential integration of (24) and after some basic algebraic manipulations, we get

$$F_{\gamma_{x_{11}}}(x) = \begin{cases}1 - \frac{\hat{\lambda}_1(a_1 - a_2 x)}{\hat{\lambda}_1(a_1 - a_2 x) + \hat{\lambda}_2 x} e^{-\frac{D_1 x}{\hat{\lambda}_1\rho(a_1 - a_2 x)}}, & x < \frac{a_1}{a_2} \\ 1, & \text{otherwise.}\end{cases} \tag{25}$$

Hence, by invoking (25) in (22), it holds

$$\bar{C}_{x_{11}} = \frac{1}{\hat{\lambda}_2 \ln 2}\int_0^{\frac{a_1}{a_2}} \frac{e^{-\frac{D_1 x}{\hat{\lambda}_1\rho(a_1 - a_2 x)}}}{(1+x)\left(\frac{x}{\hat{\lambda}_1(a_1 - a_2 x)} + \frac{1}{\hat{\lambda}_2}\right)}\mathrm{d}x. \tag{26}$$

By changing variable of $y = \frac{x}{a_1 - a_2 x}$ in (26) and after some algebraic manipulations, it occurs

$$\bar{C}_{x_{11}} = \frac{a_1\hat{\lambda}_1}{\ln 2}\int_0^\infty \frac{1}{(\hat{\lambda}_1 + \hat{\lambda}_2 y)(1 + a_2 y)(1+y)} e^{-\frac{D_1 y}{\hat{\lambda}_1\rho}}\mathrm{d}y. \tag{27}$$

If $\frac{\hat{\lambda}_2}{\hat{\lambda}_1} \neq a_2 \neq 1$, applying partial fraction decomposition in (27), we get

$$\begin{aligned}\bar{C}_{x_{11}} = \frac{a_1\hat{\lambda}_1}{\ln 2}\Bigg(&\int_0^\infty \frac{1}{(1 - \frac{a_2\hat{\lambda}_1}{\hat{\lambda}_2})(1 - \frac{\hat{\lambda}_1}{\hat{\lambda}_2})} \frac{e^{-\frac{D_1 y}{\hat{\lambda}_1\rho}}}{\hat{\lambda}_1 + \hat{\lambda}_2 y}\mathrm{d}y \\ &+ \int_0^\infty \frac{1}{(\hat{\lambda}_2 - \frac{\hat{\lambda}_2}{a_2})(1 - \frac{1}{a_2})} \frac{e^{-\frac{D_1 y}{\hat{\lambda}_1\rho}}}{1 + a_2 y}\mathrm{d}y \\ &+ \int_0^\infty \frac{1}{a_1(\hat{\lambda}_1 - \hat{\lambda}_2)} \frac{e^{-\frac{D_1 y}{\hat{\lambda}_1\rho}}}{1+y}\mathrm{d}y\Bigg).\end{aligned} \tag{28}$$

Invoking [15, Eq. (3.352.4)] in (28) we get the first branch of (8) given at the top of page 3.

On the other hand, if $\frac{\hat{\lambda}_2}{\hat{\lambda}_1}=1$, then (27) becomes

$$\bar{C}_{x_{11}}=\frac{a_1}{\ln 2}\int_0^{\infty}\frac{1}{(1+a_2y)(1+y)^2}e^{-\frac{D_1y}{\hat{\lambda}_1\rho}}\mathrm{d}y. \tag{29}$$

Applying partial fraction decomposition in (29), it occurs

$$\begin{aligned}\bar{C}_{x_{11}}=\frac{a_1}{\ln 2}\Bigg(&\int_0^{\infty}\frac{a_2^2}{a_1^2(1+a_2x)}e^{-\frac{D_1y}{\hat{\lambda}_1\rho}}\mathrm{d}y\\&+\int_0^{\infty}\frac{a_2}{a_1^2(1+x)}e^{-\frac{D_1y}{\hat{\lambda}_1\rho}}\mathrm{d}y\\&+\int_0^{\infty}\frac{1}{(1-a_2)(1+x)^2}e^{-\frac{D_1y}{\hat{\lambda}_1\rho}}\mathrm{d}y\Bigg).\end{aligned} \tag{30}$$

By applying [15, Eq. (3.352.4)] and [15, Eq. (3.353.3)], we get the second branch of (8).

Finally, if $\frac{\hat{\lambda}_2}{\hat{\lambda}_1}=a_2\neq 1$, then (27) becomes

$$\bar{C}_{x_{11}}=\frac{a_1}{\ln 2}\int_0^{\infty}\frac{1}{(1+a_2y)^2(1+y)}e^{-\frac{D_1y}{\hat{\lambda}_1\rho}}\mathrm{d}y. \tag{31}$$

Evaluating (31) similarly with (29), the third branch of (8) occurs.

In terms of $\bar{C}_{x_{12}}$, it holds

$$\bar{C}_{x_{12}}=\frac{1}{\ln 2}\int_0^{\infty}\frac{1-F_{\gamma_{x_{12}}}(x)}{1+x}\mathrm{d}x. \tag{32}$$

As a first step, we must calculate RV's $\gamma_{x_{12}}$ CDF as follows

$$\begin{aligned}F_{\gamma_{x_{12}}}(x)&=\Pr(\gamma_{x_{12}}<x)\\&=\Pr\left(\frac{a_2\rho|\hat{h}_1|^2}{\tilde{k}_1a_1\rho|\hat{h}_1|^2+\tilde{k}_2\rho|\hat{h}_2|^2+D_1}<x\right)\\&=\begin{cases}\int_0^{\infty}F_{|\hat{h}_1|^2}\left(\frac{\tilde{k}_2\rho yx+D_1x}{a_2\rho-\tilde{k}_1a_1\rho x}\right)f_{|\hat{h}_2|^2}(y)\,\mathrm{d}y, & x<\frac{a_2}{\tilde{k}_1a_1}\\1, & \text{otherwise.}\end{cases}\end{aligned} \tag{33}$$

Substituting $F_{|\hat{h}_1|^2}$, $f_{|\hat{h}_2|^2}$ and performing some algebraic manipulations, it occurs

$$F_{\gamma_{x_{12}}}(x)=\begin{cases}1-\frac{1}{1+\frac{\hat{\lambda}_2\tilde{k}_2x}{\hat{\lambda}_1(a_2-\tilde{k}_1a_1x)}}e^{-\frac{D_1x}{\hat{\lambda}_1\rho(a_2-\tilde{k}_1a_1x)}}, & x<\frac{a_2}{\tilde{k}_1a_1}\\1, & \text{otherwise.}\end{cases} \tag{34}$$

Invoking (34) in (32), we get

$$\bar{C}_{x_{12}}=\frac{1}{\ln 2}\int_0^{\frac{a_2}{\tilde{k}_1a_1}}\frac{e^{-\frac{D_1x}{\hat{\lambda}_1\rho(a_2-\tilde{k}_1a_1x)}}}{(1+x)(1+\frac{\hat{\lambda}_2\tilde{k}_2x}{\hat{\lambda}_1(a_2-\tilde{k}_1a_1x)})}\mathrm{d}x. \tag{35}$$

Changing variable of $y=\frac{x}{a_2-\tilde{k}_1a_1x}$ in (35), it follows that

$$\bar{C}_{x_{12}}=\int_0^{\infty}\frac{a_2\hat{\lambda}_1e^{-\frac{D_1y}{\hat{\lambda}_1\rho}}}{(\hat{\lambda}_1+\hat{\lambda}_2\tilde{k}_2y)(1+\tilde{k}_1a_1y)(1+(\tilde{k}_1a_1+a_2)y)}\mathrm{d}y. \tag{36}$$

It becomes apparent that (36) has a similar form with (27). Hence, for the evaluation of (36), we must take into consideration three different cases, namely

- $\frac{\hat{\lambda}_2\tilde{k}_2}{\hat{\lambda}_1}\neq\tilde{k}_1a_1\neq(\tilde{k}_1a_1+a_2)$
- $\frac{\hat{\lambda}_2\tilde{k}_2}{\hat{\lambda}_1}=\tilde{k}_1a_1\neq(\tilde{k}_1a_1+a_2)$
- $\frac{\hat{\lambda}_2\tilde{k}_2}{\hat{\lambda}_1}=(\tilde{k}_1a_1+a_2)\neq\tilde{k}_1a_1$

and perform partial fraction decomposition for each case. The above explained calculations can be executed similarly with those performed for the evaluation of (27), and thus are omitted. Following the above explained procedure, (9) given at the top of page 3 can be obtained. This completes the proof.

VI. Acknowledgments

The work of A. P. Chrysologou was supported by a PhD scholarship from the Bodossaki Foundation, Greece.

References

[1] Z. Zhang, Y. Xiao, Z. Ma, M. Xiao, Z. Ding, X. Lei, G. K. Karagiannidis, and P. Fan, "6G wireless networks: Vision, requirements, architecture, and key technologies," *IEEE Veh. Technol. Mag.*, vol. 14, no. 3, pp. 28–41, Sep. 2019.

[2] B. Clerckx, Y. Mao, E. A. Jorswieck, J. Yuan, D. J. Love, E. Erkip, and D. Niyato, "A primer on rate-splitting multiple access: Tutorial, myths, and frequently asked questions," *IEEE J. Sel. Areas Commun.*, May 2023.

[3] B. Rimoldi and R. Urbanke, "A rate-splitting approach to the Gaussian multiple-access channel," *IEEE Trans. Inf. Theory*, vol. 42, no. 2, pp. 364–375, Mar. 1996.

[4] Y. Zhu, X. Wang, Z. Zhang, X. Chen, and Y. Chen, "A rate-splitting non-orthogonal multiple access scheme for uplink transmission," in *Proc. 9th Int. Conf. Wireless Commun. Signal Process. (WCSP), Nanjing, China*, Oct. 2017, pp. 1–6.

[5] H. Liu, T. A. Tsiftsis, K. J. Kim, K. S. Kwak, and H. V. Poor, "Rate splitting for uplink NOMA with enhanced fairness and outage performance," *IEEE Trans. Wireless Commun.*, vol. 19, no. 7, pp. 4657–4670, Jul. 2020.

[6] S. A. Tegos, P. D. Diamantoulakis, and G. K. Karagiannidis, "On the performance of uplink rate-splitting multiple access," *IEEE Commun. Lett.*, vol. 26, no. 3, pp. 523–527, Mar. 2022.

[7] H. Lu, X. Xie, Z. Shi, H. Lei, N. Zhao, and J. Cai, "Outage performance of uplink rate splitting multiple access with randomly deployed users," *IEEE Trans. Wireless Commun.*, Jun. 2023.

[8] O. Abbasi and H. Yanikomeroglu, "Transmission scheme, detection and power allocation for uplink user cooperation with NOMA and RSMA," *IEEE Trans. Wireless Commun.*, vol. 22, no. 1, pp. 471–485, Jan. 2023.

[9] H. Liu, Z. Bai, H. Lei, G. Pan, K. J. Kim, and T. A. Tsiftsis, "A new rate splitting strategy for uplink CR-NOMA systems," *IEEE Trans. Veh. Technol.*, vol. 71, no. 7, pp. 7947–7951, Jul. 2022.

[10] J. Xu, O. Dizdar, and B. Clerckx, "Rate-splitting multiple access for short-packet uplink communications: A finite blocklength analysis," *IEEE Commun. Lett.*, vol. 27, no. 2, pp. 517–521, Feb. 2023.

[11] Y. Xiao, S. A. Tegos, P. D. Diamantoulakis, Z. Ma, and G. K. Karagiannidis, "On the ergodic rate of cognitive radio inspired uplink multiple access," *IEEE Commun. Lett.*, vol. 27, no. 1, pp. 95–99, Jan. 2023.

[12] S. Singh and M. Bansal, "On the outage performance of uplink NOMA inspired CR network with CEEs and imperfect SIC," in *Proc. IEEE 6th Conf. Inf. and Commun. Tech. (CICT)*. IEEE, Nov. 2022, pp. 1–5.

[13] A. P. Chrysologou, N. D. Chatzidiamantis, and G. K. Karagiannidis, "Cooperative uplink NOMA in D2D communications," *IEEE Commun. Lett.*, vol. 26, no. 11, pp. 2567–2571, Nov. 2022.

[14] S. Bisen, P. Shaik, and V. Bhatia, "On performance of energy harvested cooperative NOMA under imperfect CSI and imperfect SIC," *IEEE Trans. Veh. Technol.*, vol. 70, no. 9, pp. 8993–9005, Sep. 2021.

[15] I. Gradshteyn and I. Ryzhik, *Table of Integrals, Series, and Products*, 7th ed. New York, NY, USA: Academic, 2007.

[16] Y. Zhang, S. Feng, and W. Tang, "Performance analysis of hybrid cellular and bidirectional device-to-device cooperative NOMA communication systems," *IEEE Trans. Veh. Technol.*, vol. 70, no. 10, pp. 10 420–10 435, Oct. 2021.